Sensitivity of the Adaptive Nulling to Random Errors in Amplitude and Phase Excitations in Array Elements

Jafar Ramadhan Mohammed, Khalil Hassan Sayidmarie
College of Electronics Engineering, Nineveh University, Mosul-41001, Iraq.
jafarram@yahoo.com

***Abstract*—Adaptive antenna arrays have shown their effectiveness and powerful capabilities in modern communication and radar systems. However, maintaining this effectiveness under conditions of random errors in their element excitations is the most challenging problem. In this paper, the degradation in performance, exhibited as the elevation in the sidelobe level and changing the angular locations of the desired nulls, due to random errors in the phase and amplitude of the element excitations is investigated. First, an efficient constrained optimization approach was used to synthesize an adaptive linear array. The approach maximizes the gain in the desired direction and rejects undesired interfering signals by placing nulls towards their angles of arrivals. Then, the effects of random amplitude and phase errors in the element excitations were investigated. Simulation results showed that the nulls and the sidelobe level in the adaptive arrays are more sensitive to random errors in element phase excitations as compared to amplitude excitations.**

***Index Terms*— Adaptive Antennas; Antenna Arrays; Errors In Amplitude And Phase Excitations; Null Steering.**

I. Introduction

Performance evaluation of the adaptive antenna arrays under the influence of various errors in their excitations is an important topic and a real challenging problem in the current and future generations of the communication systems in both military and civilian applications. The adaptive antennas to be used in such systems must be characterized by a carefully controlled shape of the radiation pattern, and by nulls pointing accurately towards the directions of the interfering signals. The mainbeam shape, angular locations of the nulls, and the sidelobe level are controlled by precisely setting the amplitude and phase excitations of each array element.

In antenna arrays, the null-pointing methods are generally based on controlling; the amplitude and the phase [1-2], the amplitude-only [3], the phase-only [4], or position-only [5] of the array elements. The first method is the most expensive method considering the cost of the controllers used for both variable phase shifters and variable attenuators for each array element. The methods of amplitude-only control utilize an array of variable attenuators to adjust the element amplitudes. The phase-only null synthesis method is attractive since in a phased array, the required controls are already available for the purpose of main beam scanning [6]. The position-only control needs a mechanical driving system such as servomotors to move the array elements; thus, it is complex and costly.

In all of these aforementioned null-pointing methods, the phase shifters and attenuators are digitally controlled, and only a finite number of quantized values are available. For example, a one-bit digital phase shifter produces only two phase values of 0 and π, while a two-bit digital shifter can realize four phases of 0, $\pi/2$, π , and $3\pi/2$. Accordingly, with the use of discrete phase shifters and/or discrete attenuators, precise control over both amplitudes and phases is not possible. Therefore, unavoidable deviations (errors) in the phase and/or amplitude excitations cause some modifications of the radiation pattern from the desired one and performance degradations usually arise [7-8]. Accordingly, the nulls in the radiation pattern of the adaptive arrays may easily depart from the desired locations and then the degradation in signal-to-noise ratio performance is inevitable. Also, the accuracy of pointing a null towards an interfering signal is known to degrade substantially when considering the effect of mutual coupling between array elements [9]. Thus, there has been considerable interest in synthesizing array patterns with broad nulls [10-14] or extremely low sidelobes [2, 15] so that they can tolerate these degradations.

In [16], the effect of the frequency fluctuation on the generated nulls was investigated. A wide null at prescribed direction was achieved by subtracting a weighted pattern due to the two edge elements of the array from that of the original N-element uniform array. The proposed method provides robustness against frequency fluctuation by generating wide and deep nulls towards and around the interference directions.

In this paper, first an efficient approach based on the constrained optimization algorithm is presented to control the directionality of a single null or multiple nulls or even broad-band nulls toward the interfering directions by either controlling the amplitude-only or the phase-only of the element excitations. Then, the robustness of the above-mentioned prescribed nulls in the presence of random amplitude and phase excitation errors is investigated. The antenna radiation pattern, the null-pointing accuracy, the sidelobe level deterioration, and the main beam pointing accuracy in the presence of random errors in the element excitations are also investigated. Finally, several general conclusions are presented, accompanied by graphic displays of maximum sidelobe levels and null filling versus various error parameters.

II. Optimization Of The Linear Arrays

Consider a linear array of N=2M isotropic elements at uniformly spaced locations $x_1, x_2, \dots, x_N$, these elements are symmetrically disposed with respect to the origin along the x-axis and suppose that a harmonic plane wave with wavelength λ is incident from direction θ and propagates across the array. The N signal outputs from the array elements are weighted by the excitation coefficients w_n and summed to give the well-known linear array beam pattern [17]:

$$G(u) = \sum_{n=-M}^{M} w_n e^{jx_n u} \quad (1)$$

Where $u = \beta d sin\theta$, $\beta = 2\pi/\lambda$, $x_n = \frac{2n-sgn(n)}{2}$, sgn(n) represents the signum function, and d is the element spacing. It is required to determine the weighting vector w_n that optimizes the performance of the corresponding beam pattern, i.e., to maximize the received signal from the target direction while the sidelobes are kept below a prescribed upper bound mask. The problem is formulated as the determination of w_n such that [17]:

$$-Re[G(u)] \text{ is minimum subject to } G(u_o) = 1 \quad (2)$$

$$\text{and} \quad G(u_j) = 0 \quad j = 1,2,\dots,J$$

Where $u_o = \beta d sin\theta_o$, and θ_o is the target direction, and $u_j = \beta d sin\theta_j$, and θ_j are the directions of the interfering signals. The beam pattern under the conditions in (2) is constrained to be equal to unity at the target direction corresponding to θ_o and to reject unwanted interfering signals by placing sharp nulls in the direction of the interferers. These constraints are not sufficient to suppress wideband interfering signals. In addition, the wide nulls are required when the direction of arrival of the unwanted interfering signals is varying with time or it is not known exactly. In such cases, a comparatively sharp null has to be continuously steered to obtain a reasonable value for the signal-to-noise ratio. Therefore, further constraints for obtaining wide angular nulling are required to perform the necessary rejection of the interfering signals. Thus, (2) is rewritten to take into account a prescribed upper bound mask that introduces a wide null:

$$-Re[G(u)] \text{ is minimum subject to } |G(u_k)| < UB(u_k) \quad k = 1,2,\dots,K$$
$$\text{and } G(u_o) = 1 \quad (3)$$

where u_k is a discrete position in the farfield, and UB is a nonnegative mask function.

III. Sensitivity Of The Adaptive Nulling

A. The amplitude and phase excitation errors

From the previous section, it is clear that the vector w_n represents complex weights (i.e. amplitudes and phases). When there are random amplitude and phase errors the *nth* element weight will be:

$$w'_n = w_n(1 + \alpha_n e^{j\delta_n}) \qquad n = 1,\dots,N \quad (4)$$

where α_n is the fractional error in the amplitude weight of the *n*th element, and δ_n is the error in its phase expressed in radians. The beam pattern under these error conditions can be obtained by replacing the weighting vector w_n in (1) with w_n' of (4), to get:

$$G'(u) = \sum_{n=-M}^{M} w_n e^{jx_n u} + \sum_{n=-M}^{M} w_n \alpha_n e^{j\delta_n} e^{jx_n u} = $$
$$= G(u) + \Delta G(u) \quad (5)$$

where $G(u)$ and $G'(u)$ are the desired (i.e., error-free beam pattern) and undesired (i.e. in the presence of errors) beam patterns respectively, and $\Delta G(u)$ represents the amount of deviation from the desired beam pattern. For simplicity and clarity, all elements are assumed to be isotropic radiators, so that all changes in sidelobe levels are due to random errors in element excitation. It is also assumed that the errors have not caused any changes in the locations of the array elements.

It can be seen from (5) that the effect of the weighting error is to add an extra term to the array beam pattern. This term may dominate the sidelobes, which are far from mainbeam and may therefore seriously degrade the antenna performance in those regions. When the weighting errors, i.e., α_n and δ_n are adequately small, which is the case of practical interest, the second term $\Delta G(u)$ is generally low and will not cause noticeable changes in the mainbeam.

B. Effect of excitation errors on null accuracy

The main objective of this paper is to study the effect of the random errors in the weighting vector of the elements on the null depth and pointing accuracy. This investigation has not been previously studied to the best of author's knowledge and is of great importance in evaluating the performance of the adaptive arrays in the modern wireless communication systems. It is well-known that the optimum solution for the system described by (2) can be given by [17-18]:

$$w_{opt} = \frac{R^{-1} s(\theta_o)}{s^H(\theta_o) R^{-1} s(\theta_o)} \quad (6)$$

where R is the *N-by-N* interference-plus-noise correlation matrix, R^{-1} is the inverse of the R, and w_{opt} is the *N-by-1* optimum complex weights (i.e. in terms of both amplitude a and phase $\emptyset$)

$$w_{opt} = [a_1 e^{j\emptyset_1}, \quad a_2 e^{j\emptyset_2}, \dots, \quad a_N e^{j\emptyset_N}]^T \quad (7)$$

The *N-by-1* steering vector is defined by:

$$s(\theta_o) = [1, \quad e^{-j\theta_o}, \dots, \quad e^{-j(N-1)\theta_o}]^T \quad (8)$$

Here, the vectors are denoted in bold lower case, and matrices in bold upper case. If we now consider the random amplitude and phase errors in each element weight, then (7) can be rewritten as:

$$w'_{opt} = [a_1(1+\alpha_1)e^{j(\emptyset_1+\delta_1)}, \quad a_2(1+\alpha_2)e^{j(\emptyset_2+\delta_2)}, \dots, \quad a_N(1+\alpha_N)e^{j(\emptyset_N+\delta_N)}]^T \quad (9)$$

where α_n and δ_n are zero mean real random variables with variances $E\{\alpha_n^2\} = \sigma_\alpha^2$ and $E\{\delta_n^2\} = \sigma_\delta^2$, respectively. We also assume that the phase and amplitude errors are independent of each other. The phase and amplitude errors result in w'_{opt} deviating from w_{opt} by:

$$\Delta w = w_{opt} - w'_{opt} = [-a_1 e^{j\phi_1}(\alpha_1 + j\delta_1), \quad -a_2 e^{j\phi_2}(\alpha_2 + j\delta_2), \dots, -a_N e^{j\phi_N}(\alpha_N + j\delta_N)]^T \tag{10}$$

This deviation will result in an increase in the sidelobe level as well as errors in null-pointing. When α_n and δ_n are small, one can further simplify (10) using the approximations $cos(\delta_n) \approx 1$, $sin(\delta_n) \approx \delta_n$, and $\alpha_n \delta_n \approx 0$ so that :

$$|\Delta w|^2 = \Delta w^H \Delta w = \sum_{n=1}^{N} a_n^2(\alpha_n^2 + \delta_n^2) \tag{11}$$

The expectation of (11) yields:

$$E\{|\Delta w|^2\} = E[\sum_{n=1}^{N} a_n^2(\alpha_n^2 + \delta_n^2)] = \sum_{n=1}^{N} a_n^2(E\{\alpha_n^2\} + E\{\delta_n^2\}) = \sigma_\alpha^2 + \sigma_\delta^2 \tag{12}$$

In (12) we scale the weights so that w_{opt} has a unit norm, i.e., $\sum_{n=1}^{N} a_n^2 = 1$.

From (12), it can be seen that the mean square of the weight's deviation $E\{|\Delta w|^2\}$ is directly proportional to the mean square of the amplitude excitation errors σ_α^2 and the mean square of the phase excitation errors σ_δ^2. This means that large errors in the amplitude and/or phase excitations will result in more deviation from the optimal values. Also, note that the error in the element weight is independent of the number of array elements.

IV. Simulation Results

To evaluate the performance degradation in terms of null-pointing errors and rising sidelobe level of the linear adaptive arrays, various computer simulations have been performed under the condition of random amplitude and phase errors in the element excitations. In the following, an adaptive linear antenna array with 20 elements and half-wavelength element spacing is assumed. The induced errors in amplitude and phase are real random numbers of zero mean and *rms* values as indicated in the following examples. The error in the amplitude is expressed in relative values (-1dB corresponds to -11%), while that in the phase is expressed in absolute degrees.

As the first test example, optimization of an array pattern with constraints according to (2) is considered. Here, we assume one target and one interfering signal. The target direction is $\theta_o = 90^o$, while the interference direction is $\theta_1 = 120^o$. The error-free pattern is shown in Figure 1 by a solid black line showing the -40dB constraint of the sidelobe level. Figure 1 also shows the resulting beam patterns under various error values in the phase excitation. By comparing the error-free pattern with the distorted patterns, it is clear that the error in the phase excitation has caused a little change in the mainbeam shape, a significant change in the null position and depth, and a substantial change in the sidelobe level.

Figure 2 shows the resulting beam patterns of the same array under various error values in amplitude weights. It can be seen that the null is slightly departed from its desired location and the random amplitude errors have a significant impact on depth of the null. On the other hand, for the small values of amplitude error, there is no noticeable change in the mainbeam shape. Moreover, the effect of errors is lower than those due to the errors in the phase excitations.

The second test example has considered three interfering signals arriving from the directions; $\theta_1 = 45^o$, $\theta_2 = 60^o$, and $\theta_3 = 140^o$ respectively, while the target direction is the same as in the previous examples. Figure 3 shows the resulting beam patterns under various errors in phase excitation, while Figure 4 shows the resulting beam patterns under various errors in amplitude excitation. It is clear from Figure 3 that the random errors in the phase of the weights result in the filling of the nulls (Here, the depth of the first null at $\theta_1 = 45^o$and the third null at $\theta_3 = 140^o$ have both changed from -100 dB to -30 dB, and the depth of the second null at $\theta_2 = 60^o$ has changed from -100 dB to -20 dB). Thus, the adaptive array under such condition is unable to effectively suppress the interference signals. The filling of the desired nulls is much lower with the case of random errors in amplitude. Here, although the angular locations of the desired nulls at $\theta_1 = 45^o, \theta_2 = 60^o, \theta_3 = 140^o$ are not greatly affected, the depth of these nulls has changed from -100dB to -60 dB, yet they are still low.

In the third test example, the linear array is optimized according to (3) to provide a pattern that has depression (wide angular null) of width 20^ocentered at 140^o. The wide angular null can be introduced by imposing prescribed upper bound (mask) constraint on the sidelobe level. The mask is shown in Figure 5 and Figure 6, where the level of the depression is constrained to be less than -70 dB. For ∓ 0.5 dB error in amplitude weights, the level of the depression is slightly increased to -60dB, whereas $\mp 5^o$ error in phase excitation has increased the level of the depression to -30dB. From the above test examples, it can be concluded that the use of amplitude-only control for null steering in adaptive arrays provides less sensitivity to the random errors in the element weights.

Next, the depth of the desired null at 120^o and the peak level of the sidelobe are plotted as a function of errors in amplitude and phase weights (see Figure 7 and Figure 8). Clearly, the depth of the null and the peak sidelobe are changing more rapidly under the condition of phase errors as compared to the case of amplitude errors.

Finally, the effect of random errors in the amplitude and phase weights is considered. Figure 9 shows the random variations in the amplitude weights of the array elements, while Figure 10 shows the random variations in the phase weights. For comparison, the ideal (error-free) amplitude and phase weights are also included. Note that these element weights are corresponding to the array radiation patterns that are shown in Figure 1 and Figure 2 respectively. From Figures 9 and 10 and according to (5) and (11), it can be seen that the higher random errors in the amplitude and/or phase weights, the larger are the deviations from the error-free values of the array pattern. Also, the errors on the amplitude and/or phase weights cause noticeable increasing in the SLL and all the tunable nulls will depart from their desired directions.

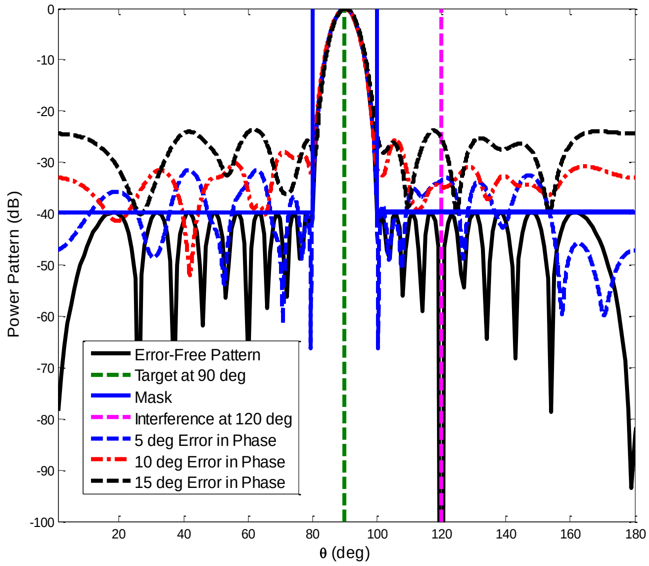

Figure 1: Effect of random phase errors on the adaptive nulling for N=20 elements, and a single null at 120 deg.

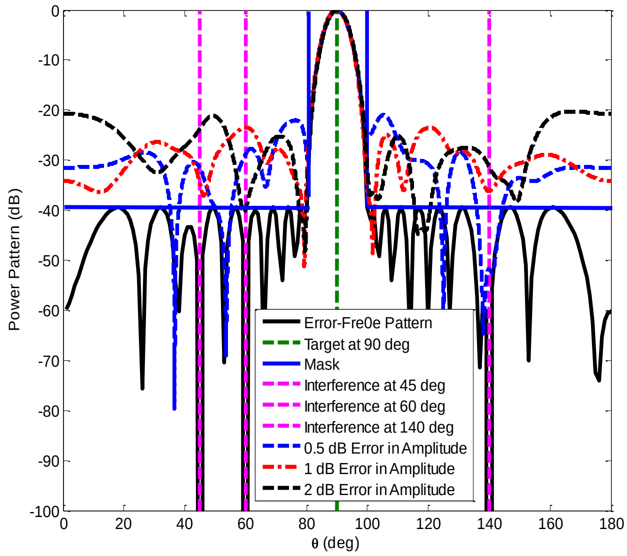

Figure 4: Effect of random errors in the array amplitude on the adaptive nulling for *N*=20 elements, and three nulls at 45, 60, and 140 deg.

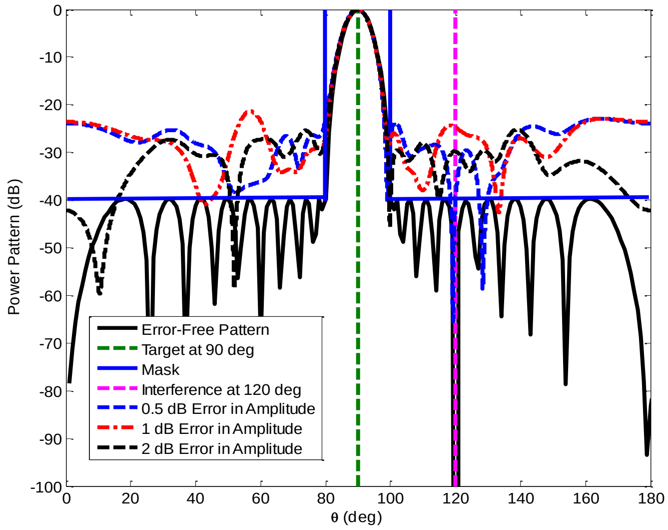

Figure 2: Effect of random amplitude errors on the adaptive nulling for N=20 elements, and a single null at 120 deg.

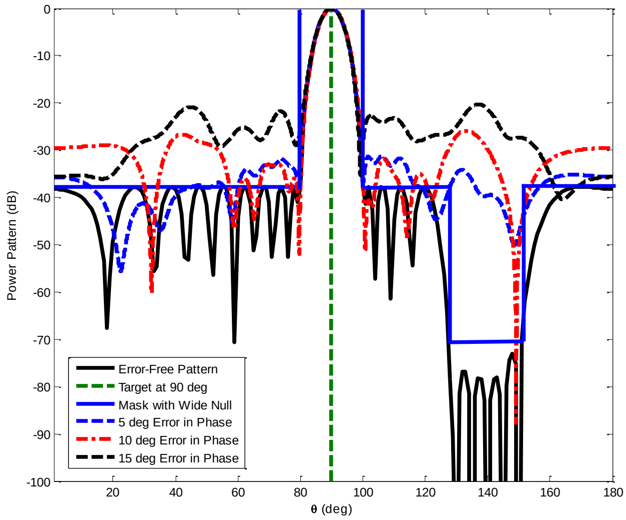

Figure 5: Effect of random errors in the array phases on the adaptive nulling for *N*=20 elements, and wide null around 140 deg.

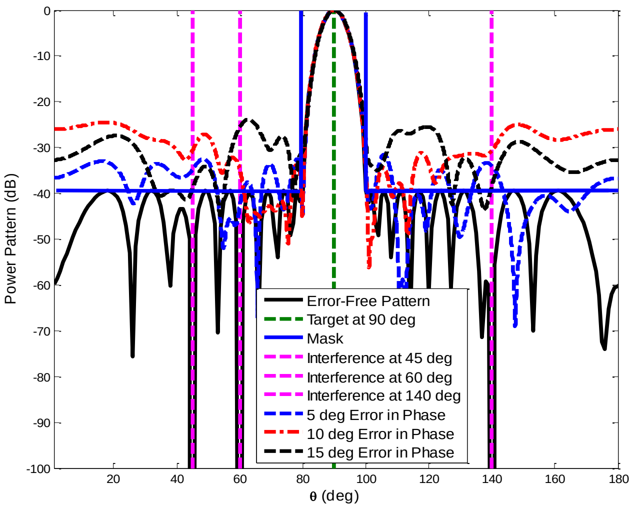

Figure 3: Effect of random errors in the array phases on the adaptive nulling for N=20 elements, and three nulls at 45, 60, and 140 deg.

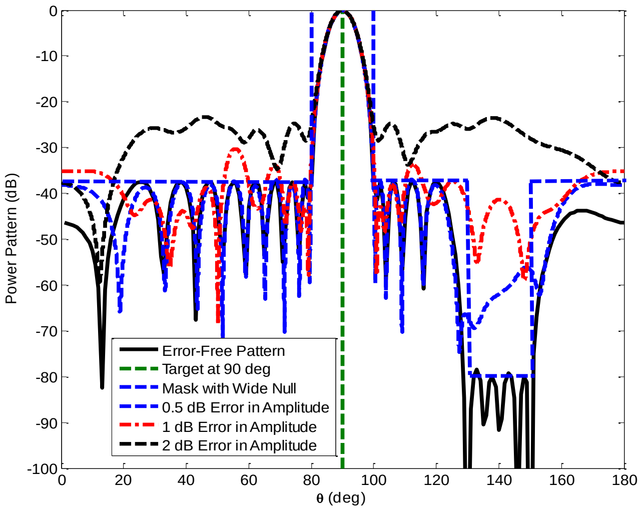

Figure 6: Effect of random errors in the array amplitude on the adaptive nulling for N=20 elements, and wide null around 140 deg.

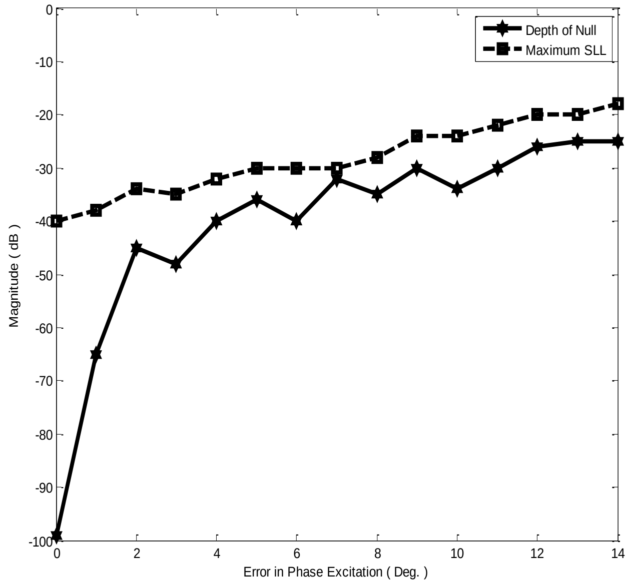

Figure 7: The depth of the null and the peak sidelobe level versus random errors in phase excitation.

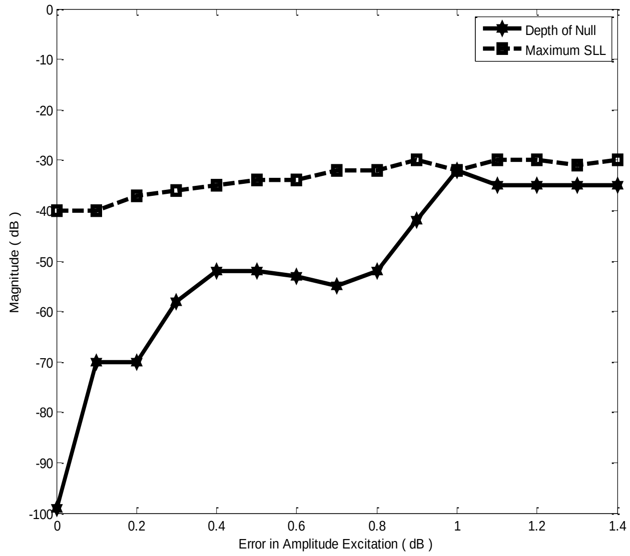

Figure 8: The variation of the null depth and the peak sidelobe level versus random errors in amplitude weights.

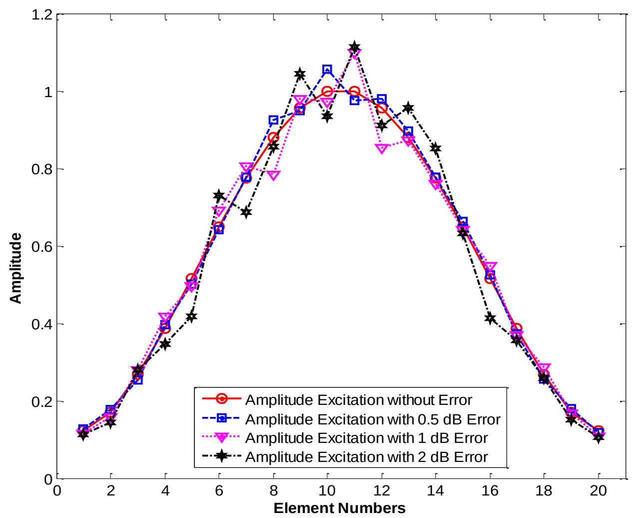

Figure 9: The arrays weights for various levels of error in the amplitude.

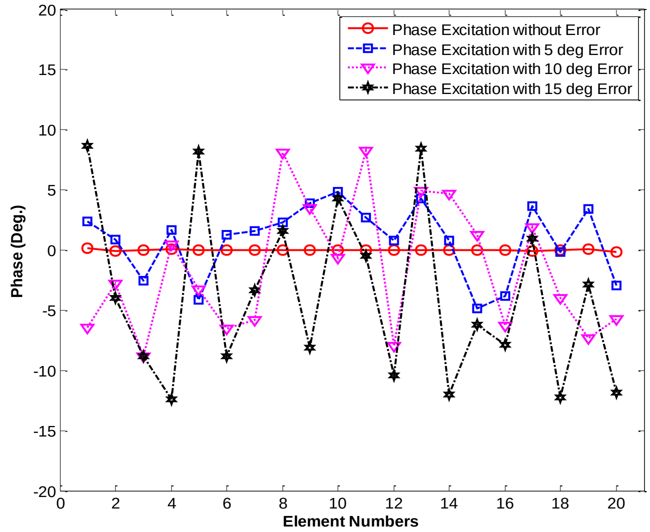

Figure 10: The phases of the array weights for various levels of error in the phase

V. CONCLUSIONS

It has been shown that the random errors present in the weights of an adaptive array can degrade its performance. Performance degradation includes an increase in the sidelobe level, changing the main-beam shape, null filling and deportations from desired directions. From the simulation results, it can be seen that the effect of random phase errors is substantially greater than that of random amplitude errors. Moreover, the simulation results have shown that, if the errors do not take large values, the beam-pointing error is negligible.

To prevent such a circumstance, the adaptive antenna arrays must be accurately calibrated before being employed in the real-world applications. This is especially true for large phased array space-based radar antennas, for which anti-jam performance is critical, and no maintenance work can be done once deployed in orbit.

This study can be further extended to employ an interval analysis method [19] to precisely predict the deviation in the null positions and peak sidelobe level.

REFERENCES

[1] Peter J. Bevelacqua and Constantine A. Balanis, "Minimum Sidelobe Levels for Linear Arrays," IEEE Trans. Antennas Propag., vol. 55, No. 12, pp. 3442-3449, December 2007.

[2] Mohammed, J. R., “Phased Array Antenna with Ultra-Low Sidelobes”, Electronics Letters, Vol. 49, Issue 17, pp. 1055-1056, August 2013.

[3] Lopez, P., Rodriguez, J. A., Ares, F. and Moreno, E., “Low Sidelobe Level In Almost Uniformly Excited Arrays”, Electron. Lett., Vol. 36, No. 24, pp. 1991-1993, 2000.

[4] Haupt, R. L., "Phase-Only Adaptive Nulling with a Genetic Algorithm," IEEE Trans. on Antennas and Propagat., Vol. 45, No. 6, 1009-1015, 1997.

[5] A. Tennant, M.M. Dawoud, and A.P. Anderson, "Array Pattern Nulling By Element Position Perturbations Using A Genetic Algorithm", Electron Lett., Vol. 30, pp. 174–176, 1994.

[6] Ghayoula, R., Fadlallah, N., Gharsallah, A. and Rammal, M.," Phase-Only Adaptive Nulling With Neural Networks For Antenna Array Synthesis", IET Microw. Antennas Propag., 2009, Vol. 3, Issue 1, pp. 154–163

[7] Keizer, W. P. M. N. , "Low Sidelobe Phased Array Pattern Synthesis with Compensation for Errors Due to Quantized Tapering", IEEE Trans. Antennas Propagat., Vol.59, No. 12, pp. 4520-4524, Dec. 2011.

[8] Pozar, D. M., and Kaufman, B., "Design Considerations for Low Sidelobe Microstrip Arrays", IEEE Trans. Antennas Propagat., Vol. 38, No. 8, pp. 1176-1185, Aug. 1990.

[9] Fei Zhao, Huiying Qi, Ke Xiao, Lei Qiu, and Shunlian Chai, "The Experimental Study of Mutual Coupling in Conformal Array", Microwave and Optical Technology Letters, Vol. 54, No. 1, January 2012.

[10] Mohammed, J. R. and Sayidmarie, K. H., "A New Technique for Obtaining Wide-Angular Nulling in the Sum and Difference Patterns of Monopulse Antenna", IEEE Antennas and Wireless Propagation Letters, Vol.11, pp. 1242-1245, 2012.

[11] Mohammed, J. R., "Design of Printed Yagi Antenna with Additional Driven Element for WLAN Applications", Progress in Electromagnetics Research C, Vol. 37, 67-81, January 2013.

[12] Mohammed, J. R. and Sayidmarie, K. H., "A Null Steering Method By Controlling Two Elements", IET Microwaves, Antennas & Propagation, Vol. 8, Issue 15, PP. 1348-1355, 2014.

[13] Mohammed, J.R.," Optimal Null Steering Method in Uniformly Excited Equally Spaced Linear Array by Optimizing Two Edge Elements", Electronics Letters, Vol. 53, Issue 11, May 2017.

[14] Mohammed, J.R and Sayidmarie, K. H., "Performance Evaluation of the Adaptive Sidelobe Canceller with various Auxiliary Configurations," AEÜ International Journal of Electronics and Communications, Vol. 80, pp. 179–185, 2017.

[15] Mohammed, J.R and Sayidmarie, K. H., "Synthesizing Asymmetric SideLobe Pattern with Steered Nulling in Non-uniformly Excited Linear Arrays by Controlling Edge Elements," International Journal of Antennas and Propagation, Vol. 2017, Article ID 9293031, 8 pages, 2017.

[16] Sayidmarie, K. H. and Mohammed, J. R., "Performance of a Wide Angle and Wideband Nulling Method for Phased Arrays", Progress in Electromagnetics Research M, Vol. 33, pp. 239-249, October 2013.

[17] Li, J. and Stoica, P., "Robust Adaptive Beamforming", John Wiley and Sons, Inc., Hoboken, New Jersey, 2006.

[18] Yang, K., Zhao, Z., and Liu, Q. H. ,"Robust Adaptive Beamforming Against Array Calibration Errors", Progress In Electromagnetics Research., PIER. 140, pp. 341-351, 2013.

[19] Hansen, E. and Walster, G. W., "Global Optimization Using Interval Analysis", New York, NY: CRC Press, 2004.